

*Development and Characterization of Bioactive Polyethylene-Glycol-Polylactic-Acid  
Membranes for Colorimetric Glucose Sensing*

A Thesis

Presented to the Faculty of the College of Human Ecology  
of Cornell University

in Partial Fulfillment of the Requirements of the  
Undergraduate Honors Program

By

Antonio P. Martinez

April 2021

© 2021 Antonio P. Martinez

## **ABSTRACT**

Polyethylene glycol and polylactic acid bioactive membranes were developed for glucose sensor applications. Polylactic acid and polyethylene glycol were co-axially electrospun into a nonwoven, nanofibrous membrane composed of a core-sheath fiber structure. Differential scanning calorimetry and confocal microscopy were respectively utilized to confirm the polymer composition and fiber structure of the electrospun membrane. To create the bioactive membrane for glucose sensing, a bienzyme system and colorimetric agent were encapsulated in the polyethylene-glycol-polylactic-acid fiber structure. By encapsulating horseradish peroxidase and glucose oxidase in the polyethylene glycol core and *o*-dianisidine in the polylactic acid sheath of the fiber, immersion in glucose solutions causes the oxidized colorimetric agent to diffuse into the solution, allowing for colorimetric measurement with the glucose solution. UV-vis spectroscopy confirmed successful glucose sensing, showcasing a linear relationship in absorbance at 440 nm and mM concentration of glucose solution with a 90% activity retention with the membrane. The stability of the polyethylene-glycol-polylactic-acid bioactive membrane was found to be dependent on storage time at room temperature: activity of the membrane reduced to 79% approximately 2 months after fabrication. Future directions for this experiment include optimization of the electrospinning process to reduce needle-tip blockage from unspun polymer solution, or ‘icing’, and the reduction of the diffusion time for colorimetric glucose detection.

## **BIOGRAPHICAL SKETCH**

Antonio P. Martinez was born in El Centro, California on September 15<sup>th</sup>, 1999. Antonio graduated from Central Union High School in June of 2017. In August of 2017, he began his Bachelor of Science degree at Cornell University as a Fiber Science major in the department of Fiber Science and Apparel Design in the College of Human Ecology. He began working on his thesis project with Professor Margaret Frey in May of 2020. In May of 2021, he will receive a Bachelor of Science degree from the Fiber Science program.

## **ACKNOWLEDGEMENTS**

First and foremost, I am extremely grateful to Dr. Margaret Frey for her support and guidance in the last two years, not only on this thesis but also throughout my journey through academia. This thesis would not have been possible without her lessons and advice. I am also grateful to the Fiber Science and Apparel Design faculty for all of their help and making my academic experience at Cornell so memorable. I am also thankful to the members of Professor Frey's research group for their advice, generosity and their company when working in the lab.

Finally, I cannot express enough gratitude towards my family for everything they have done for me. Thank you to my parents, to whom this thesis is dedicated, to my sisters, Tessa and Tali, for their valuable opinions and willingness to help whenever they could and for always being there to support me.

## **TABLE OF CONTENTS**

CHAPTER 1: INTRODUCTION .....	11
1.1 <i>Diabetes mellitus</i> .....	11
1.2    Membrane-based Glucose Sensors .....	12
CHAPTER 2: LITERATURE REVIEW .....	14
2.1    Glucose Sensors .....	14
2.2    Co-axial Electrospinning .....	15
2.3    Polylactic Acid (PLA) & Polyethylene Glycol (PEG) .....	18
2.3.1    Polylactic Acid.....	18
2.3.2    Polyethylene Glycol.....	18
2.3.3    Coaxial Electrospinning of PLA & PEG .....	19
2.4    Active Agents for Glucose Detection .....	20
2.5    An Innovative Step in Membrane-based Biosensor Progress.....	21
CHAPTER 3: EXPERIMENTAL PROCEDURE.....	23
3.1    Materials .....	23
3.1.1    Materials for Membrane Preparation .....	23
3.1.2    Materials for Glucose Testing.....	24
3.1.3    Instruments for Membrane Characterization .....	24
3.2    Fabrication of PLA/PEG Membranes.....	24
3.2.1    Electrospinning of Individual Polymer Solutions.....	24
3.2.2    Co-axial Electrospinning .....	25
3.3    Characterization of PLA/PEG Membranes.....	27
3.3.1    Digital Scanning Calorimetry .....	27

3.3.2	Confocal Microscopy.....	27
3.4	Testing for Optical Glucose Exposure.....	28
3.4.1	Preparation of Glucose Solutions.....	28
3.4.2	Testing with Glucose Solutions .....	28
3.4.3	UV-vis Spectroscopy .....	29
CHAPTER 4: RESULTS AND DISCUSSION.....		30
4.1	Electrospinning of Individual Polymer Solutions.....	30
4.1.1	Polylactic Acid.....	30
4.1.2	Polyethylene Glycol.....	31
4.2	Co-Axial Electrospinning of PLA-PEG with Dye Markers .....	32
4.3	Initial Characterization.....	33
4.3.1	Digital Scanning Calorimetry .....	33
4.3.2	Confocal Microscopy.....	35
4.4	Co-Axial Electrospinning of Loaded PLA-PEG.....	38
4.5	Testing for Optical Glucose Exposure.....	39
4.5.1	Optical Results .....	39
4.5.2	UV-vis Spectroscopy .....	41
CHAPTER 5: CONCLUSIONS .....		49
CHAPTER 6: FUTURE DIRECTIONS.....		51
APPENDIX .....		53
REFERENCES .....		61

## **LIST OF FIGURES**

FIGURE 2.1	Illustration of co-axial electrospinning procedure for core-sheath fibers..	16
FIGURE 2.2	Illustration of property combinations done with co-axial electrospinning	17
FIGURE 2.3	Cross-sectional view of an electrospun PLA-PEG hollow-fiber membrane.....	19
FIGURE 2.4	Overview of the reaction mechanism for GOx, HRP, and o-dianisidine...	20
FIGURE 2.5	Schematic illustration of setup for co-axial electrospinning ‘ready-to-use’ membrane.....	21
FIGURE 2.6	Schematic illustration of co-axial electrospinning set-up for PEG-PLA membrane.....	22
FIGURE 3.1	Digital image of colorimetric testing of PEG-PLA Membranes approximately 5 minutes after immersion .....	28
FIGURE 4.1	Digital and light microscopic image of a membrane with 15% PLA concentration (trial 9 from table 4.3) .....	31
FIGURE 4.2	Digital and light microscopic image of a membrane with 17% PEG concentration (trial 10 from table 4.4). .....	32
FIGURE 4.3	Digital and light microscopic image of PEG-PLA membrane (trial 10 from table 4.5). .....	33
FIGURE 4.4	DSC graph of a PEG-PLA membrane (trial 9 in table 4.5) .....	34
FIGURE 4.5	Confocal microscopic images of a PEG-PLA membrane (0.75 mL core flow rate) using 10x magnification lens (trial 1 from table 4.6) .....	36
FIGURE 4.6	Confocal microscopic images of a PEG-PLA membrane (0.85 mL core flow rate) using 10x magnification lens (trial 2 from table 4.6) .....	36



FIGURE 4.7 X-Z axis orthogonal view of a PEG-PLA membrane (0.75 mL core flow rate, trial 1 from table 4.6) .....	37
FIGURE 4.8 X-Z axis orthogonal view of a PEG-PLA membrane (0.85 mL core flow rate, trial 2 from table 4.6) .....	37
FIGURE 4.9 Digital image of PEG-PLA membrane (trial 3 from table 4.7) .....	39
FIGURE 4.10 24-hour testing of PEG-PLA in 5 mL glucose solutions (trial 3 from table 4.7) .....	39
FIGURE 4.11 2 mL glucose solutions after exposure to PEG-PLA membrane (trial 4 from table 4.7) for 10 minutes .....	40
FIGURE 4.12 2 mL glucose solutions from figure 4.11 after 24 hours.....	41
FIGURE 4.13 Absorbance of free-enzyme glucose solutions across wavelength range of 500 to 350 nm for calibration purposes. ....	42
FIGURE 4.14 Calibration curve for absorbance at 440 nm of free-enzyme glucose solution concentrations .....	43
FIGURE 4.15 Calibration curve for absorbance at 440 nm of varying glucose solution concentrations exposed to PEG-PLA membrane.....	44
FIGURE 4.16 Absorbance at 440 nm for varying glucose solutions exposed to a 60-day-old, 30-day-old, and 1-day-old PEG-PLA membrane .....	47
FIGURE 4.17 Activity rate of PEG-PLA membrane samples over storage time .....	48

## **LIST OF TABLES**

TABLE 4.1	Electrospun PLA Mats of varying concentrations .....	53
TABLE 4.2	Electrospun PEG mats of varying concentrations .....	54
TABLE 4.3	Electrospinning 15% PLA solutions with varying parameters .....	55
TABLE 4.4	Electrospinning 17% PEG solutions with varying parameters .....	56
TABLE 4.5	Co-axial electrospinning PLA and PEG solutions.....	57
TABLE 4.6	Co-axial electrospinning PLA and PEG solutions with fluorescent dyes .....	58
TABLE 4.7	Co-axial electrospinning PLA and PEG solutions with HRP, GOx, & <i>o</i> - dianisidine .....	58
TABLE 4.8	Co-axial electrospinning PEG-PLA membranes for colorimetric testing .....	59
TABLE 4.9	Absorbance at 440 nm for glucose solutions exposed to PEG-PLA membranes from table 4.8-1,2,3 .....	59
TABLE 4.10	Absorbance at 440 nm for glucose solutions exposed to stored PEG-PLA membranes from table 4.8-4,5 .....	60

# **CHAPTER 1**

## **INTRODUCTION**

This thesis focuses on the development and characterization of polyethylene glycol (PEG)-polylactic acid (PLA) fiber membranes functionalized with a bienzyme system and colorimetric agent for optical glucose detection. The experiment discussed in this thesis consists of two parts: first, the production of the fiber membranes to encapsulate the bienzyme system and colorimetric agent, and second, the testing of these membranes with immersion/exposure to aqueous glucose solutions. The exploration of electrospinning methodology and the characterization of the fiber membranes formed are discussed throughout this thesis. Additionally, the significance of these nanofiber biosensors is discussed, as this field of research has potential to increase the range of materials that could be used in making biodegradable and noninvasive options for biosensing. The need for biodegradability in biosensors is increasing—healthcare facilities in the United States generate almost 3,500 tons of waste each day [1].

### ***1.1 Diabetes mellitus***

Diabetes mellitus refers to a group of metabolic disorders describing an abnormal level of blood sugar, glucose, over an extended period of time [2][3]. Around the globe, diabetes affects almost 400 million people and was the seventh leading cause of death in the United States in 2017 [3]. As of now, the most common method of glucose monitoring/sensing for those with diabetes is a blood sugar meter, that uses a testing strip immobilized with enzymes targeted at glucose oxidation and uses a meter to measure the electricity that passes through that strip [2]. Many alternative approaches to glucose sensing have been extensively researched over time; in the context of academic research,

Senthamizhan et al. have thoroughly reviewed glucose sensors based on electrospun nanofibers and divided these research efforts into two broad fields: enzymatic sensing and non-enzymatic sensing [4]. Much research within these areas is focused on expanding the range of materials for glucose sensing by traversing into using new materials and agents for detection.

## **1.2 Membrane-based Glucose Sensors**

Electrospun fibers have been a promising host material for creating glucose sensors both enzymatically and nonenzymatically. In comparison to common nanomaterials for glucose detection such as nanospheres, nanotubes, or other nanostructures, there are a number of avenues that can be taken with electrospun fibers for glucose detection. One can use electrospun fibers to replace other base materials such as to maximize the efficiency of or aid in the process for electrochemical meters by replacing the substrate which glucose is exposed to, or it can be fabricated to be the glucose sensor itself [4]. Electrospun nanofibers are of interest due to their increased flexibility in comparison to other nanostructures; they allow for the integration of the active agents through in-situ (placing the agents in the solutions before electrospinning) or ex-situ (attaching the molecules onto the surface of the electrospun nanofibers) approaches [4].

Electrospun fibers as glucose sensors have been shown to be versatile in that when fabricated without defect, they can hold various advantages and are capable of encapsulating specific active agents for functionalization to certain stimuli detection [4]. The incentive for using electrospun fibers is their wide range of application in their mechanical properties and their ability to be engineered to desired specifications.

Specifically, this thesis seeks to create a PEG-PLA bioactive membrane for applications in colorimetric biosensing of glucose.

## **CHAPTER 2**

### **LITERATURE REVIEW**

#### **2.1 Glucose Sensors**

Enzymatic glucose sensors are those that use enzymes, notably glucose oxidase ( $GO_x$ ), to oxidize and detect glucose in the fluid being measured [2][4]. The fluids used for these sensors are typically biomedically-related (i.e. sweat, blood, etc), but these sensors may work on any fluid containing glucose depending on any extraneous contaminants in testing fluid [2][4]. Common contaminants include triglycerides, oxygen, and uric acid, all of which are found in body fluids [6]. Enzymatic glucose sensors have a significantly higher selectivity of glucose due to the presence of an enzyme targeted towards glucose oxidation. Another available enzyme is glucose dehydrogenase, which has been commercially used for commercial blood glucose detection devices, but the enzyme is associated with high costs and the accompanying need for adenosine triphosphate [4]. Glucose oxidase is advantageous for its relatively low cost and accessibility, and much academic work involving glucose sensors has focused on this enzyme [4]. While the better selectivity of enzymatic glucose sensors compared to non-enzymatic glucose sensors, there are still challenges associated with enzymatic glucose sensors, such as the possibility of denaturation due to differences in pH and temperature during measurement [4].

Non-enzymatic glucose sensors are those that do not use an enzyme to catch glucose, and instead rely on electro-catalysts for glucose selectivity [4]. Despite not relying on an enzyme for glucose detection, there are significant challenges to overcome with non-enzymatic glucose sensors: these sensors have limited sensitivity in detecting glucose due to the low kinetics in regards to the glucose electro-oxidation on electrodes, and have poor

selectivity of glucose due to the possible oxidation of extraneous sugars and other interfering compounds within the fluid being measured for glucose [4].

Due to these challenges, the enzymatic approach will be taken for this project. As of now, little research has been published dealing with an enzymatic glucose sensor using strictly an electrospun membrane that relies on detection through purely colorimetric means. One paper has been published using the redox reaction of a colorimetric agent, *o*-diansidine, and bienzyme system, GOx and HRP, to induce optical color change of the membrane [6]. This project seeks to contribute to this field by developing a PEG-PLA bioactive membrane with the same mechanism.

## **2.2 Co-axial Electrospinning**

Electrospinning has been on the rise as a means of encapsulating enzymes and other chemical agents for nanofiber functionalization, as biomolecules and other agents can be immobilized onto these nanofibers [7]. Electrospinning is defined as the uniaxial elongation of a jet, released from the charged polymer solution in the presence of a strong electric field [8]. Subsets of electrospinning include coaxial electrospinning, which involves an arrangement of two concentric spinnerets meant to co-spin polymer solutions to generate nano- to micro-sized fibers with varying structures [8]. Notably, core-sheath fibers can be produced using co-axial electrospinning, in which two polymer solutions are extruded with two concentric spinnerets [8][9]. A diagram of co-axial electrospinning for core-sheath fibers can be seen in Figure 2.1.

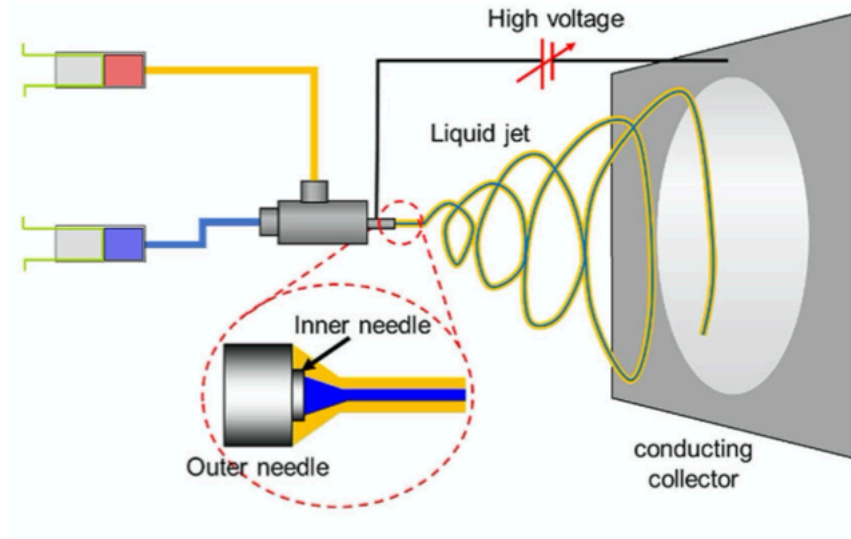


**Figure 2.1.** Illustration of co-axial electrospinning procedure for core-sheath fibers [9].

The use of a core-sheath structure in co-axial electrospinning allows for individual polymer solutions to encapsulate their own components to create a composite fiber with combined properties of not only the two polymers, but agents encapsulated as well [9]. If two agents are not soluble in the same solution, there is opportunity to separate them into individual polymer solutions. A schematic illustration of the potential combinations for properties using coaxial electrospinning can be seen in Figure 2.2.



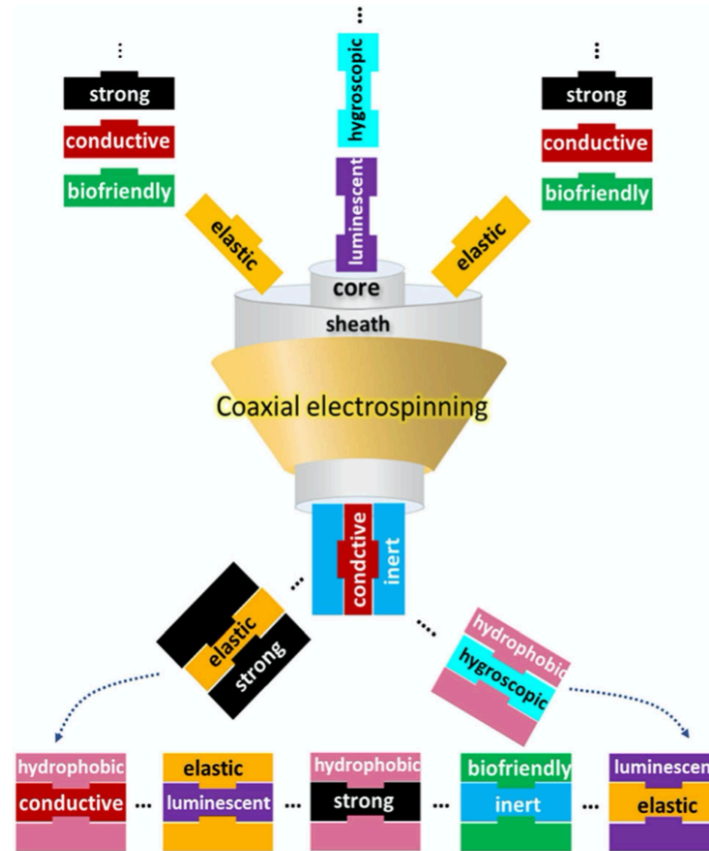


**Figure 2.2.** Illustration of property combinations done with co-axial electrospinning [9].

With co-axial electrospinning, one can intertwine properties of two unlike polymers, creating composite fibers with a breadth of characteristics [8][9]. Moreover, co-axial electrospinning can be used to make polymers with low spinnability have increased more spinnable by using a polymer much more spinnable, bringing opportunity for polymers that are unspinnable individually [9]. In the context of this experiment, two properties being combined are biodegradability and cost-efficiency, as PLA has a high level of spinnability and PEG is known for its biocompatibility. These properties are discussed in further detail below.

## **2.3 Polylactic Acid & Polyethylene Glycol**

### **2.3.1 *Polylactic Acid (PLA)***

PLA is a biodegradable and biocompatible polymer that is often manufactured for biomedical purposes in the context of electrospinning [10]. Moreover, PLA is well-known for having great spinnability with a number of conventional solvents [10]. In the context of the biomedical field, electrospun PLA is most often targeted towards drug delivery and tissue scaffold applications [10][11]. With that, common reported properties of electrospun PLA include good mechanical strength, high surface area, and cost-efficiency [10]. Research with PLA and glucose sensors thus far has been limited to enzymatic glucose sensors that rely on electrodes [4]. Currently, there is no literature regarding the use of PLA in glucose sensors that rely on strictly enzymes and colorimetric agents for measurement. For this study, PLA was chosen for its excellent spinnability and ability to be spun with the colorimetric *o*-dianisidine.

### **2.3.2 *Polyethylene Glycol (PEG)***

Similar to PLA, PEG is another highly biocompatible and biodegradable polymer often used in the biomedical field [12]. PEG is the lower molecular weight variation (<5000 Da) of polyethylene oxide, and has shown to be a popular companion for other polymers in either polymer blends and/or composites [12]. Currently, research regarding the use of PEG in glucose sensors is also limited to enzymatic sensors involving electrodes [13], and there is a lack of research regarding its use in colorimetric-based enzymatic sensors. For this study, PEG was chosen for its biocompatibility and ability to be spun with the enzymes GOx and HRP.

### 2.3.3 Previous Work in Co-axial Electrospinning PLA-PEG

Research on co-axial electrospinning with PLA and PEG is minimal, but has potential for many fields due to its notable features when co-axially spun [11][13]. More specifically, Pant et al. thoroughly reviewed the drug delivery applications of core-sheath nanofibers and found that PEG-PLA and co-axial electrospinning has focused on bio-scaffolds for tissue applications similar to their individual applications [13]. Ou et al. had a notable observation when coaxial electrospinning PEG-PLA for a hollowed-out core-sheath structure; there was an epitaxial-like membrane created at that ability to be highly-aligned in the electrospinning process [11]. To do this, a rotating drum was used to collect the electrospun fibers to create a membrane that followed the alignment of the underlying fibers as it was spinning, and washing to remove its PEG core [11]. In doing so, the authors found increased mechanical properties and alignment.

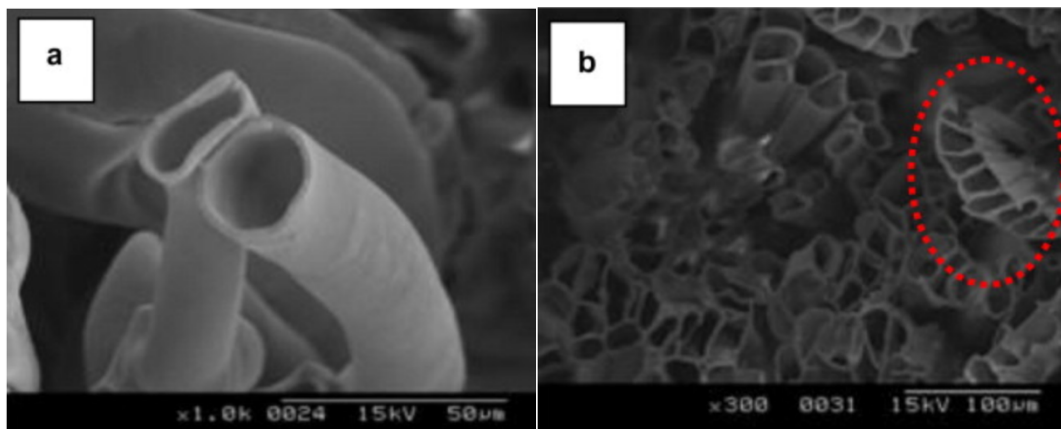


**Figure 2.3.** Cross-sectional view of the electrospun PLA-PEG hollow-fiber membrane, showing (a) two single hollow fibers and (b) a bundle of hollow fibers with an average diameter of 20–30  $\mu\text{m}$  and a wall thickness of a few microns [11].

It is important to note however that these papers do not research the inclusion of any active agents in the core and sheath components of the membrane; instead, these papers served as

reference for developing a coaxial electrospinning methodology for PEG-PLA. Although the experiment for this thesis does not use a rotating drum for membrane collection, there is potential for increased alignment in PEG-PLA electrospun membranes alone, which would inherently improve the mechanical strength of the membrane collected.

## 2.4 Active Agents for Glucose Detection

In previous literature, the bienzyme system of glucose oxidase (GOx) and horseradish peroxidase (HRP) and colorimetric agent of *o*-dianisidine has been shown to be a successful medium to detect glucose in enzymatic glucose sensors [3][12]. GOx and HRP are well-known assays for beta-D-glucose, and are often coupled with colorimetric agent(s) for optical glucose sensing [4][6]. *O*-dianisidine is a colorless peroxidase substrate that is often used to measure lactate or glucose, and has great stability in comparison to other agents used with this bienzyme system [6]. The reaction mechanism between the coenzymes and colorimetric agent can be seen in Figure 2.4.

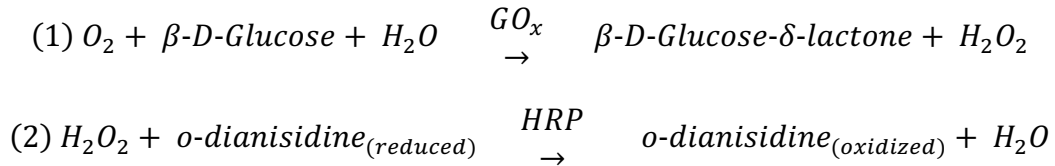


**Figure 2.4.** Overview of the reaction mechanism for GOx, HRP, and *o*-dianisidine [6].

With this mechanism, their sensors typically rely on colorimetric glucose sensing with or without electrodes [4]. This reaction mechanism has been incorporated into materials (nanofibers, nanospheres, nanotubes) for glucose sensing through microfluidics or entrapment through co-axial electrospinning or cross-linking [4][14][15]. Glucose oxidase denatures outside of a pH range of 4-7 and temperatures below or past 0-10 degrees Celsius. Horseradish peroxidase denatures outside of a pH range of 5-9 and temperatures below or past -20 to -10 degrees Celsius.

## 2.5 Using PLA-PEG Membrane for Glucose Sensing

Based on the literature examined previously, PLA and PEG are suitable materials for glucose sensors due to their cost-effectiveness, spinnability, and biocompatibility. With these materials, co-axially electrospun PEG-PLA core-sheath membranes were functionalized for glucose detection. To create this membrane, the bienzyme system of HRP and GOx was encapsulated in the PEG core and the colorimetric agent, *o*-dianisidine, was encapsulated in the PLA sheath. A similar methodology was explored using polyurethane and glycerol to create a co-axially electrospun hollow nanofiber membrane for colorimetric glucose sensing [6]. A schematic illustration of Ji's experiment can be seen in Figure 2.5.

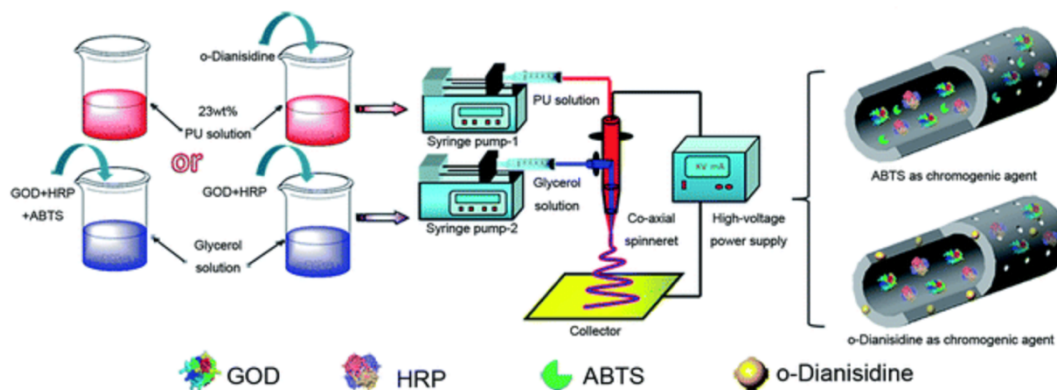


**Figure 2.5.** Schematic illustration of setup for co-axial electrospinning ‘ready-to-use’ membrane [6].

This paper served as the grounds for the methodology of this experiment, however, the PEG-PLA structure was not hollowed out; instead a core-sheath fiber membrane was created. By creating this PEG-PLA bioactive membrane with the bienzyme system and colorimetric agent, the membrane can allow for the colorimetric detection of glucose in solutions based on the diffusion of the colorimetric agent out of the fibers. In doing so, the

solutions can be quantitatively measured using UV-vis spectroscopy, and possibly optically measured with a standardized colorimetric scale. A schematic illustration of this experiment can be seen in Figure 2.6.

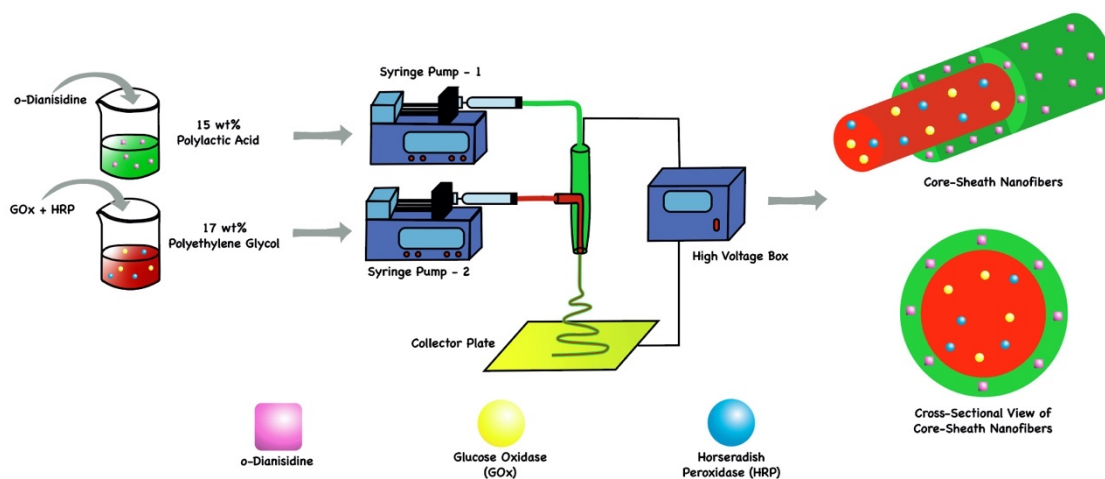


**Figure 2.6.** Schematic illustration of co-axial electrospinning set-up for PEG-PLA membrane.

This work seeks to broaden and showcase the availability of common materials that can be used as enzymatic glucose sensors. The simplicity in co-axial nanofiber membrane production and advantages in purely colorimetric sensing open the door for further development of these glucose sensors.

## **CHAPTER 3**

### **EXPERIMENTAL PROCEDURES**

#### **3.1 Materials**

##### ***3.1.1 Materials for PLA/PEG Membrane Preparation***

PLA pellets supplied from *JAMPLAST* (4043D) were used as the sheath polymer for coaxial electrospinning. PEG supplied from *Sigma Aldrich* was used as the core polymer for this experiment. Reagent-grade dichloromethane (DCM) supplied from *Sigma Aldrich* and ACS-grade dimethylformamide (DMF) supplied from *Fisher Chemical* were used as the solvents for the PLA solution, and deionized water was used as the solvent for the PEG solution. GOx and HRP were supplied from *TCI America* and *Alfa Aesar* respectively, to be used as the enzymes to detect glucose in the core of the fibers. O-dianisidine was supplied from *Beantown Chemical* to be used as the colorimetric agent in the sheath of the fibers. Rhodamine-B and Coumarin-6 were supplied from *Santa Cruz Biotechnology* to be used as the fluorescent dyes for confocal microscopy characterization. Sourcing of all these materials were supported by the grant: HATCH multi-state project NC1194 Nanotechnology and Biosensors.

A pre-built electrospinning needle with 22-gauge and 18-gauge concentric needle spinneret was supplied from *Rame-hart Instruments* for co-axial electrospinning. PTFE tubing was also supplied from *Rame-hart Instruments* for polymer solution extrusion in the co-axial needle. Syringe pumps supplied from *Harvard Apparatus* and *KD Scientific* were used to facilitate co-axial electrospinning.

### ***3.1.2 Materials for Glucose Testing of PLA/PEG Membranes***

Beta-D-Glucose was supplied from *MP Biomedicals* to create the glucose solutions of various concentrations. Phosphate-buffered saline (PBS) packets were supplied from *VWR International* to be used as the solvent for the glucose solutions. All of these glucose solutions were made in 5-mL or 20-mL scintillation vials.

### ***3.1.3 Instruments for PLA/PEG Membrane Characterization***

The compositions of the fiber membranes were characterized using differential scanning calorimetry (DSC, Q200, TA Instruments). The morphologies of the fibers were characterized using light microscopy (BX51, Olympus) and confocal microscopy (CLSM, LSM880, Zeiss). Colorimetric detection of glucose was characterized using UV-vis spectroscopy (UV-vis, Lambda 35, Perkin Elmer).

## **3.2 Fabrication of PLA/PEG Membranes**

### ***3.2.1 Electrospinning of Individual Polymer Solutions***

PLA and PEG polymer solutions were individually electrospun to explore and identify parameters to be used in co-axial electrospinning. PLA and PEG polymer solutions were prepared individually in 20-mL scintillation vials. PLA solutions (10 mL) were made using a 9:1 solvent of DCM to DMF. The PLA concentrations in the solutions varied from 10% to 17% weight. PEG solutions (10 mL) were made using distilled water. The PEG concentrations in the 6 solutions varied from 10% to 17% weight. The solutions were stirred or shaken for approximately 24 hours for complete dissolution. The first set of trials included spinning the varying concentrations of PLA and PEG solutions at 1 mL/hr for 30 min at 20 kV, with the collecting plate at 15 cm from the needle of the syringe. These results can be found in Tables 4.1 and 4.2 at the appendix respectively. The electrospinning



parameters were based on previous work reported in the literature [6]. After identifying spinnable concentrations, a second set of trials was conducted varying the parameters of electrospinning. This involved changing the needle-to-plate distance and/or voltage. A 21-gauge needle and a 5 mL syringe were used for all trials. These results can be found in Tables 4.3 and 4.4 at the appendix respectively.

### ***3.2.2 Co-axial Electrospinning of PLA/PEG Membranes***

PLA and PEG polymer solutions were co-axially electrospun to create the fiber membrane. Optimal parameters were identified, and agents were loaded into the nanofiber membrane for characterization and testing. PLA and PEG polymer solutions were prepared individually in 20-mL scintillation vials. PLA solutions (10 mL) at 15% weight concentration were made using a 9:1 solvent of DCM to DMF. PEG solutions (10 mL) at 17% weight concentration were made using distilled water. The solutions were stirred or shaken for approximately 24 hours for complete dissolution. To create the nanofiber membrane, the PLA solution was used in the sheath needle and PEG solution was used in the core needle. Trials were conducted varying the flow rates for these polymer solutions with a 12 cm needle-to-plate distance and 15 kV for 30 minutes. Both solutions were colorless, and created white membranes when electrospun. One to two drops of green food coloring were added to the core polymer solution to colorimetrically differentiate core and sheath solutions in the membrane. The membranes were left to dry for approximately 24 hours after electrospinning. The observations from these experiments can be found in Table 4.5 in the appendix. The membranes were characterized for composition using DSC.

The second set of trials included loading fluorescent dyes in the core and sheath solutions for characterization in confocal microscopy. 15% PLA (10 mL) solutions were

prepared and approximately 1.0 mg of Rh-B was incorporated into the solutions. 17% PEG solutions (10 mL) were prepared and approximately 1.0 mg of C-6 was incorporated into the solutions. The amounts for fluorescent dyes were identified from previous literature [14]. These dyes were added immediately after the polymer pellets were added into 24 hours. The parameters for electrospinning included a sheath flow rate of 1 mL/hr and core flow rate of 0.75 or 0.85 mL/hr, with a 12 cm needle-to-plate distance and 15 kV for 30 minutes. The membranes were fabricated and then were characterized using confocal microscopy. The membranes were left to dry for approximately 24 hours after electrospinning. The observations from these experiments can be found in Table 4.6 in the appendix.

The third set of trials focused on loading the active ingredients in the core and sheath solutions. 15% PLA solutions (10 mL) were prepared and approximately 20-40 mg of *o*-dianisidine were incorporated into the solution. 17% PEG solutions (10 mL) were prepared and approximately 5-8 mg of GOx and 5-8 mg of HRP were incorporated into the solution. These solutions were prepared based on a 4 mg *o*-diansidine to 0.5 mg HRP and GOx ratio. The proportion for the colorimetric agent and bienzyme system were taken from previous literature [12]. These agents were added and stirred for approximately 10 minutes in the solvent before their respective polymer pellets were added, and the solutions were shaken and/or stirred for approximately 24 hours. The membranes were then fabricated and observed for spinnability. The parameters for electrospinning included a sheath flow rate of 1 mL/hr and core flow rate of 0.75 mL/hr, with a 12 cm needle-to-plate distance and 15 kV for 30 minutes. The membranes were left to dry for approximately 24 hours after

electrospinning. The observations from these experiments can be found at Table 4.7 in the appendix.

For colorimetric testing, a ratio of 20 mg of *o*-dianisidine to 2.5 mg of GOx and HRP was used to fabricate the bioactive membranes. This ratio was identified based on the third set of trials [16]. The parameters for electrospinning included a sheath flow rate of 1 mL/hr and core flow rate of 0.75 mL/hr, with a 12 cm needle-to-plate distance and 15 kV. Each membrane was spun for approximately 10 minutes to obtain approximately 15 mg of the membrane for testing. Each membrane was allowed to dry for 24-hours after spinning, and was placed in storage at ambient temperature after 24 hours.

### **3.3 Characterization of PEG-PLA Membranes**

#### **3.3.1 *Differential Scanning Calorimetry (DSC)***

Approximately 1.5 mg of the PEG-PLA sample were loaded into the DSC instrument for characterization. DSC was conducted with a heating rate of 20 degrees Celsius/min. Once the data was collected, the melting peaks were characterized for enthalpy of heat, onset temperature, and peak temperature.

#### **3.3.2 *Confocal Microscopy***

Microscopy images were obtained with a 10x water-immersion magnification lens. The sheath polymer was excited using an argon laser at the wavelength of 458 nm for coumarin-6. The core polymer was excited at the wavelength of 561 nm for rhodamine B. The wavelength channel for coumarin-6 was green at excitation and for rhodamine B, it was red. To analyze the microscopy images, the image processing software, *FIJI*, was used to characterize core-sheath fiber size and diameters and identify 2D, 3D, and orthogonal views.

### 3.4 Testing for Optical Glucose Exposure

#### 3.4.1 Preparation of Glucose Solutions

A stock 200-ml 50 mM phosphate-buffer saline was made. Using this stock buffer solution, various 5-mL beta-D-glucose solutions were made of exponential concentration up to 1 mM (i.e. 0 mM, 0.001 mM, 0.01 mM, 0.1 mM, 1 mM) in 20-mL scintillation vials. To generate a calibration curve with UV-vis spectroscopy, beta-D-glucose solutions were made in intervals of 0.02 mM from 0 to 0.1 mM.

#### 3.4.2 Testing with Glucose Solutions

Based on previous literature [6], the ratio for bioactive membrane to glucose solution was 1 mL glucose solution to 3 mg bioactive membrane. For the 5-mL glucose solutions, 15 mg of the bioactive PLA-PEG core-sheath membrane was immersed in each solution for 10 minutes. After 10 minutes, the bioactive membrane was removed from each solution and placed in a separate scintillation vial. These glucose solutions were then tested using UV-vis spectroscopy. Digital images of the solutions were taken before and after exposure to bioactive membrane.

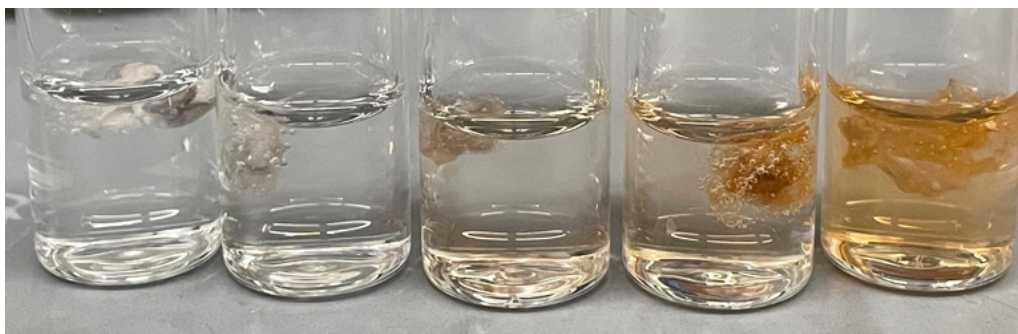


**Figure 3.1.** Digital image of colorimetric testing of PEG-PLA Membranes approximately 5 minutes after immersion.

### 3.4.3 *UV-vis Spectroscopy*

To examine absorbance across a wavelength range, the glucose solutions in each trial were scanned for absorbance from 500-350 nm. Absorbances were also recorded at maximal absorbance for *o*-diansidine, which was reported to be at 440 nm [6]. Graphs were made for the data collected were made using *Origin* graphing software.

## **CHAPTER 4**

### **RESULTS AND DISCUSSION**

#### **4.1 Electrospinning of Individual Polymer Solutions**

The first set of trials for PLA and PEG were focused on finding the optimal concentration for spinnability. The assessment for these trials was based on visual consistency of fibers and light microscopy.

##### ***4.1.1 Polylactic Acid***

For PLA, the spinnability of the polymer increased with concentration up to 15%. When spinning at 17%, the PLA web was noticeably less concentrated on the collecting plate. Moreover, the samples with concentrations at 10-12% also had low collection rates when being spun. In comparing two PLA membranes fabricated with 15% PLA concentration (table 4.1, trial 5) and 17% PLA concentrations (table 4.1, trial 7) under the light microscope, it was clear that the membrane made with a 15% PLA concentration had bead-free nanofibers. For the membrane with a 17% PLA concentration, there was a small bit of beading in the nanofibers, and this can most likely be attributed to the higher concentration of PLA being spun onto the plate. For these reasons, a 15% PLA polymer solution was selected for PLA solution concentrations going forward.

In the second set of trials for PLA, it was determined that a lessened distance for the needle-to-plate and voltage allowed for improved spinnability. When increasing the voltage and/or distance, the solution had an increased level of blockage at the needle tip due to polymer build-up from evaporated solvent, also known as icing, at the needle tip. When decreasing the voltage and/or distance, the icing was minimal, but at a certain point, the needle began to spray the polymer solution onto the collecting plate. The point at which

spinning PLA was optimal had a 12 cm needle-to-plate distance and a 15 kV voltage. A PLA sample electrospun with the parameters identified in the last two set of trials can be seen in Figure 4.1.



**Figure 4.1.** Digital (left) and light microscopic (right) image of a membrane with 15% PLA concentration (trial 9 from table 4.3).

#### ***4.1.2 Polyethylene Glycol***

For PEG, the spinnability of the polymer increased with concentration to 17%. PEG was less spinnable than PLA. When spinning at 17%, the PEG web was noticeably more concentrated on the collecting plate than previous concentrations spun, but there was still a steady level of spraying. Although spraying was present, it was not a concern due to the spinnability of PLA, which would increase the spinnability of PEG when co-axially electrospun. In comparing all samples of PEG under the light microscope, it was clear that the 17% sample was the best, despite having minimal web formation. For these reasons, a 17% PEG polymer solution was selected for PEG solution concentrations going forward.

In the second set of trials for PEG, it was also determined that a decreased distance for the needle-to-plate and decreased voltage resulted in improved spinnability. Similar spinning behavior occurred with PEG as for PLA; if the voltage and/or distance were increased or decreased too much, PEG would respectively either ice or spray. Similar to

PLA, the point at which spinning PEG was optimal had a 12 cm needle-to-plate distance and a 15 kV voltage. A PEG sample electrospun with the parameters identified in the last two set of trials can be seen in Figure 4.2.



**Figure 4.2** Digital (left) and light microscopic (right) image of a membrane with 17% PEG concentration (trial 10 from table 4.4).

#### **4.2 Co-Axial Electrospinning of PLA-PEG with Dye Markers**

The first trials for PLA and PEG were focused on finding the correct flow rates for each solution. Based on previous literature, it was known that the sheath flow rate would be higher than that of the core flow rate, thus experiments focused on identifying this gap [5][6]. Immediately, it was noticed that increasing the flow rate of PLA was detrimental to the electrospinning process, as much icing occurred once this rate exceeded 1 mL/hr. The collected webs also showcased a minimal level of green, indicating that the core of PEG was not being created. This was also evidenced with the leakage of the PEG solution at the needle tip. These results led experiments to focus on lowering the core flow rate, and better results were collected. When spinning at a flow rate of 0.75 mL/hr for the core solution, it was noticed that the green color was much more present on the collected web. In comparison to the 0.85 mL/hr flow rate, the color was more identifiable. A digital and



microscopic image of the PEG-PLA membrane spun with a core flow rate of 0.75 mL/hr (trial 10 from table 4.5) can be seen in Figure 4.3.

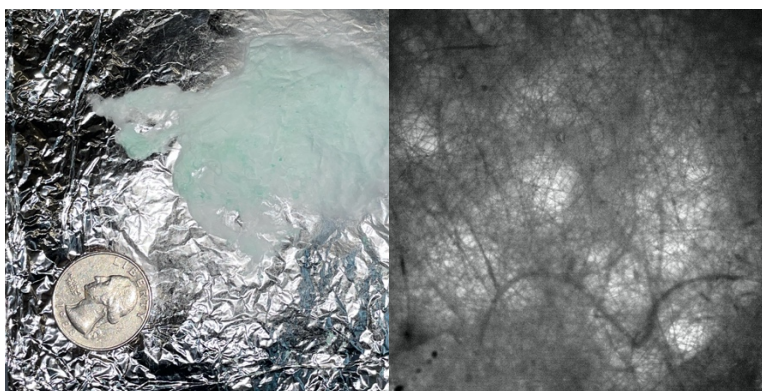


**Figure 4.3.** Digital (left) and light microscopic (right) image of PEG-PLA membrane (trial 10 from table 4.5).

### **4.3 Initial Characterization**

#### ***4.3.1 Differential Scanning Calorimetry***

Samples from table 4.5 were also characterized for composition using DSC to validate the inclusion of both PLA and PEG in the nanofiber web. The graph of one sample measured with DSC can be seen in Figure 4.4. Looking at the graph, it is clear that both PLA and PEG are present in the nanofiber web spun with a sheath flow rate of 1.0 mL/hr and core flow rate of 0.75 mL/hr. From literature, the melting points of PLA and PEG are respectively 155 and 62 degrees Celsius [10][12]. The collected melting peaks at 61.56 and 151.78 degrees Celsius aligned with these melting points, signifying that both polymers are present. The gap between the melting points was large enough to not question the identities of the polymers in question.

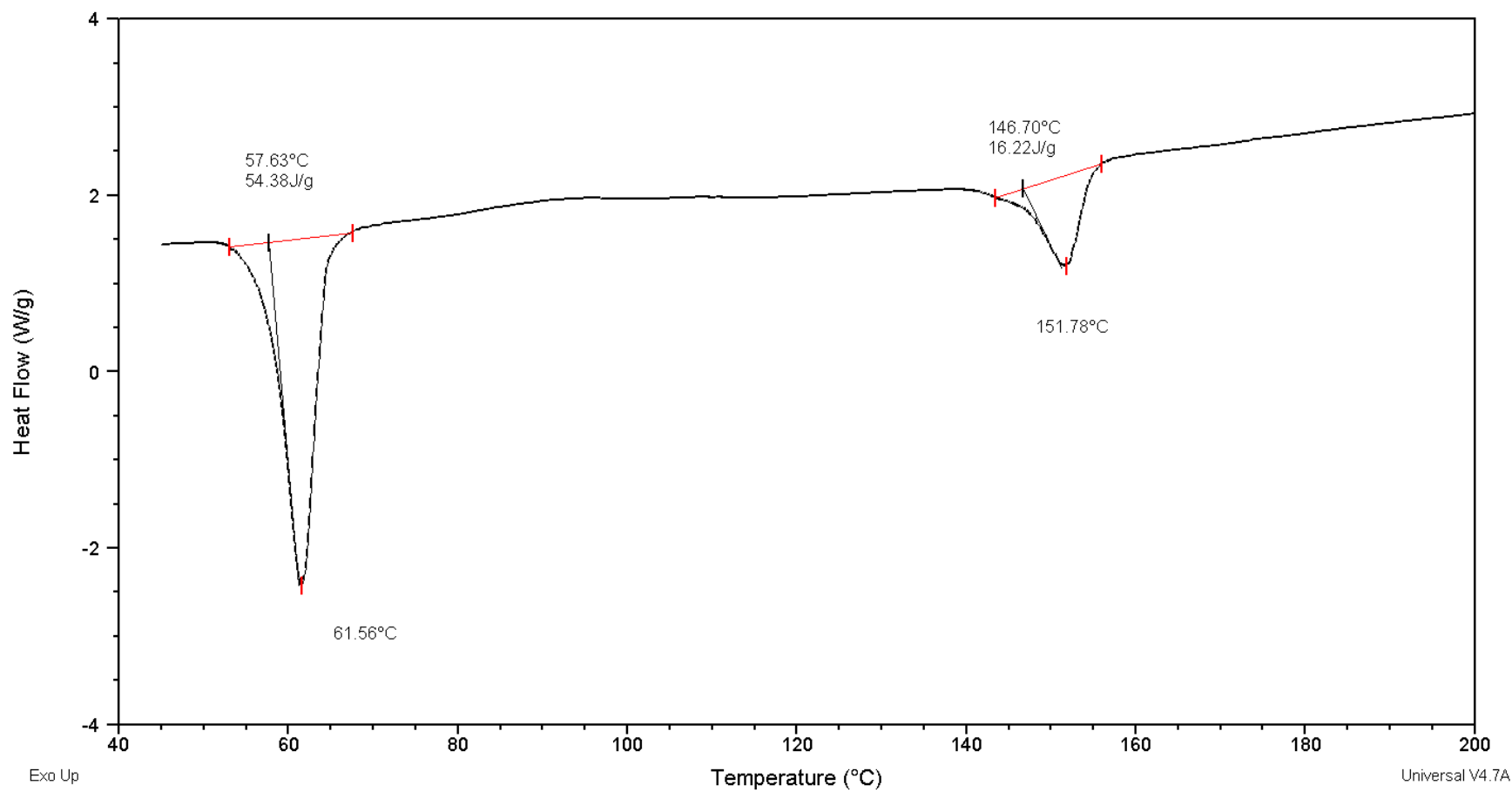


**Figure 4.4.** DSC graph of a PEG-PLA membrane (trial 9 in table 4.5).

### ***4.3.2 Confocal Microscopy***

Based on the results of the first trials, two samples with different core flow rates at 0.75 mL/hr and 0.85 mL/hr were made and loaded with fluorescent dyes. A digital image of the PEG-PLA membrane made using a 0.75 mL/hr core flow rate, trial 1 from table 4.6, can be seen in Figure 4.5. The microscopy images for samples with varying core flow rates of 0.75 and 0.85 mL/hr can be seen in Figures 4.5 and 4.6.

Looking at the images collected with confocal microscopy, it was clear that both polymers were present in the nanofiber web, and that the core flow rate of 0.75 mL/hr produced the best core-sheath structure. Comparing the composite images between the two samples, trial 1 (table 4.6) had much more yellow fluorescence, signifying the presence of both dyes in the sample, whereas the concentration of the yellow fluorescence for trial 2 (table 4.6) was not as significant. The yellow fluorescence in the composite image for trial 1 (table 4.6) was also more uniform along the fiber, and the yellow fluorescence color in sample 4.6-2 was more disconnected. Looking at the individual images for the sheath and core structures, sample 4.6-1 had much better uniformity through the fibers, and sample 4.6-2 had little-to-no concentration in some areas of the sample. As far as fiber diameter, the diameter of the collected fibers were approximated to be 15 micron on average, with the core diameter being approximated at 10 micron and sheath diameters approximated at 15 micron thick. To ensure that the core-and-sheath fibers were being created, an orthogonal view, or view from the X-Z axis, of each sample was examined. The views for the PEG-PLA membranes (trials 1 and 2 from table 4.6) can be seen in Figures 4.7 and 4.8.

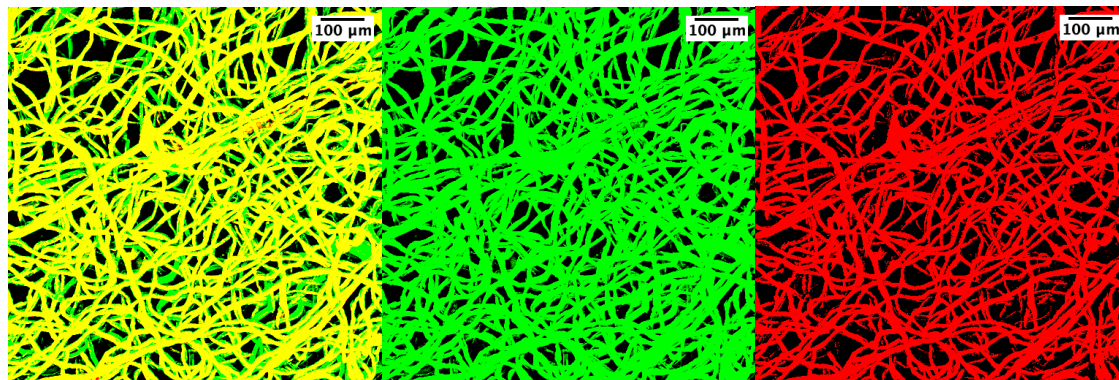


**Figure 4.5.** Confocal microscopic images of a PEG-PLA membrane (0.75 mL core flow rate) using 10x magnification lens (trial 1 from table 4.6). Left image was composite of PLA and PEG dyes, middle image was PLA (sheath), and right image was PEG (core).

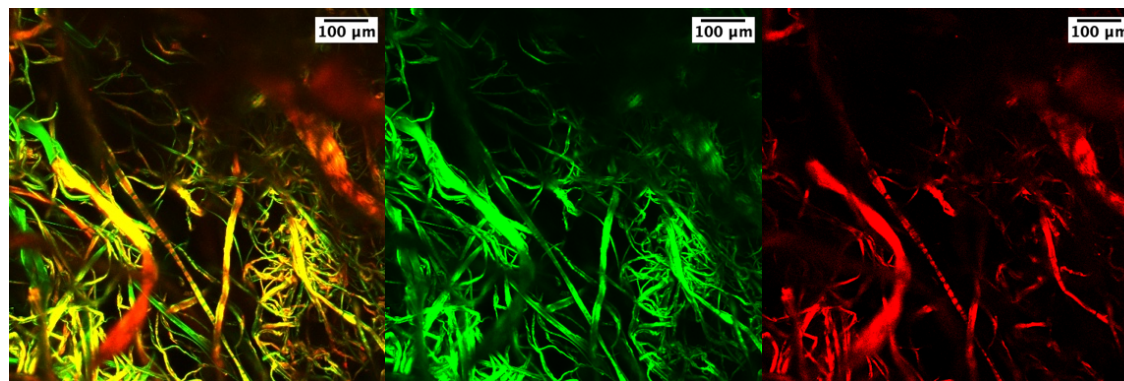


**Figure 4.6.** Confocal microscopic images of a PEG-PLA membrane (0.85 mL core flow rate) using 10x magnification lens (trial 2 from table 4.6). Left image was composite of PLA and PEG dyes, middle image was PLA (sheath), and right image was PEG (core).

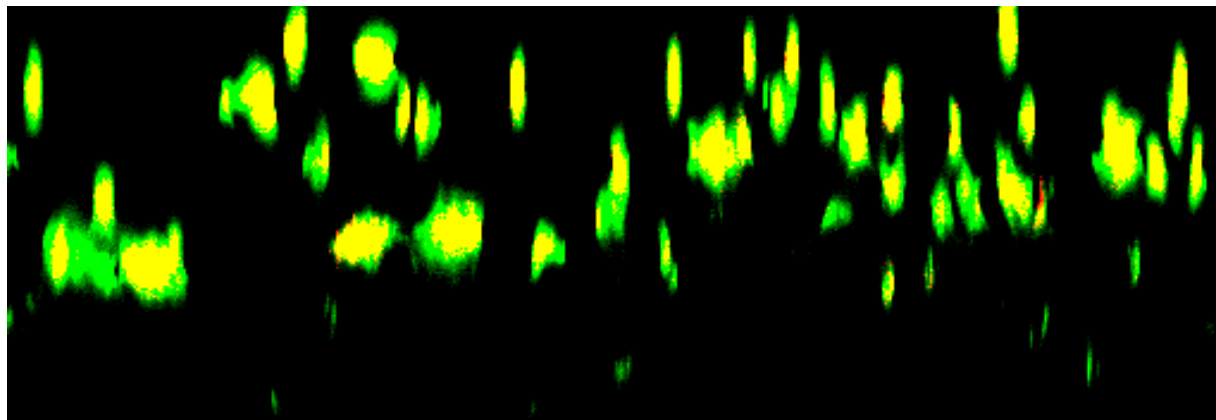


**Figure 4.7.** X-Z axis orthogonal view of a PEG-PLA membrane (0.75 mL core flow rate, trial 1 from table 4.6).

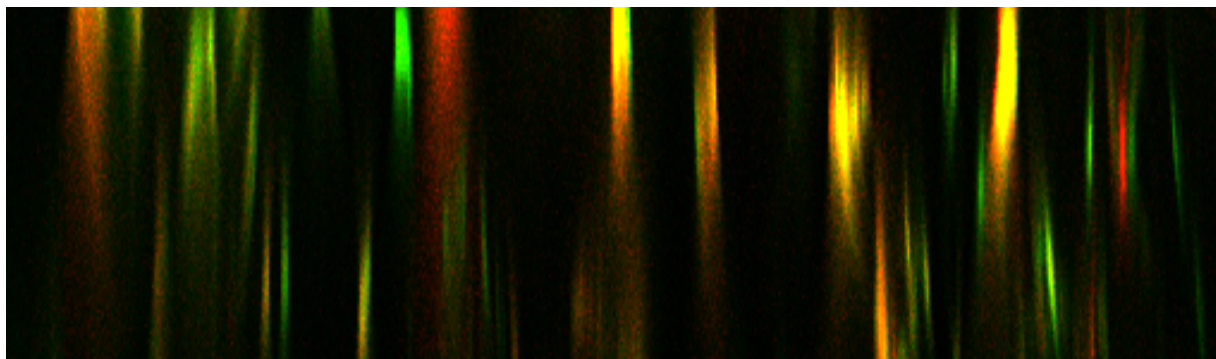


**Figure 4.8.** X-Z axis orthogonal view of a PEG-PLA membrane (0.85 mL core flow rate, trial 2 from table 4.6).

Looking at the orthogonal views, the PEG-PLA membrane using a 0.75 ml/hr core flow rate (trial 1 from table 4.6) had clear core-sheath fiber structures. The PEG-PLA sample made with a 0.85 mL/hr flow rate (trial 2 in table 4.6) did not have as distinct structures, and the colors presented in this view are heavy in red fluorescence. The increase in red fluorescence signified that there was inconsistent coverage of the core with the sheath polymer, as it would fluoresce yellow if it were fully covered. With these results, it was decided that 0.75 mL/hr would be the ideal flow rate for the PEG solution when co-axial electrospinning.

#### **4.4 Co-Axial Electrospinning of Loaded PLA-PEG**

When spinning with active ingredients, it was noted that *o*-dianisidine was not as soluble in the PLA solution as anticipated, as the solution was more of a suspension. The added 20 to 40 mg of *o*-dianisidine significantly increased the viscosity of the PLA solution, causing much icing at the co-axial needle tip at amounts past 20 mg, as indicated by the poor spinning of samples using 30 and 40 mg *o*-dianisidine. These observations for these trials are recorded in table 4.7 in the appendix. Upon increased icing at the needle tip when increasing concentration of the *o*-dianisidine in the PLA solution, little to no amounts of PEG-PLA membrane were collected. Based on the results of this set of trials, a 20 mg *o*-dianisidine and 5 mg HRP/GOx amount used for colorimetric testing. A digital image of the PEG-PLA membrane spun with a core flow rate of 0.75 mL/hr (trial 10 from table 4.5) can be seen in Figure 4.9.

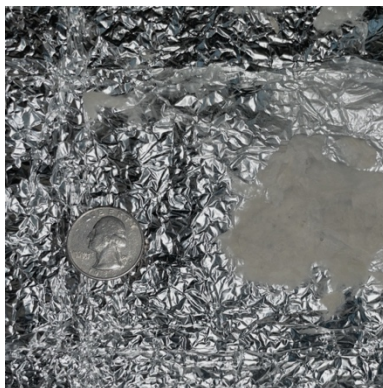


**Figure 4.9.** Digital image of PEG-PLA membrane (trial 3 from table 4.7).

## 4.5 Testing for Optical Glucose Exposure

### 4.5.1 Optical Results

An initial 24-hour test was conducted using a PEG-PLA membrane holding 20 mg of *o*-dianisidine and 5 mg of HRP and GOx (sample 3 from table 4.7). A digital image can be seen in Figure 4.10 of a test at 24 hours.



**Figure 4.10.** 24-hour testing of PEG-PLA in 5 mL glucose solutions (trial 3 from table 4.7). Concentrations from left to right are 0, 0.001, 0.01, 0.05, 0.1 mM.

Looking at the color intensities, it appeared that the intensities appear in an increasing linear gradient optically, meaning that the reaction mechanism finished in or under 24-hours. Theoretically, if the glucose oxidase and horseradish peroxidase, or *o*-dianisidine were the limiting reagents, one would see equivalent color intensities across concentrations. However, because the intensities are increasing optically with

concentration, it was clear that the glucose solution was limiting the mechanism. Upon initial observation of the testing, it was noticed that there was a visibly linear gradient in color intensity at approximately 10 minutes. Due to this observation, this time frame for the remainder of colorimetric testing was chosen. Another test was conducted using a second sample of the same active agent amounts (sample 4 from table 4.7). A digital image can be seen of the test after 10 minutes of exposure with the nanofiber sample in Figure 4.11.

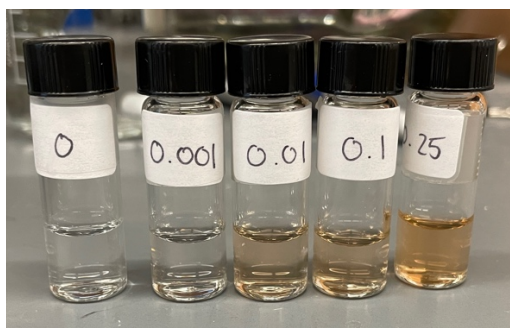


**Figure 4.11.** 2 mL glucose solutions after exposure to PEG-PLA membrane (trial 4 from table 4.7) for 10 minutes. Concentrations from left to right are 0, 0.001, 0.01, 0.1, 0.25 mM.

The color change was apparent at 10 minutes with this test, and the intensities of these colors increased with glucose concentration. After removing the membranes, the solutions were left for 24 hours to examine any further color change to see if there was a diffusion of the bienzyme system into the solution. A digital image of the solutions after 24-hours can be seen in Figure 4.12.



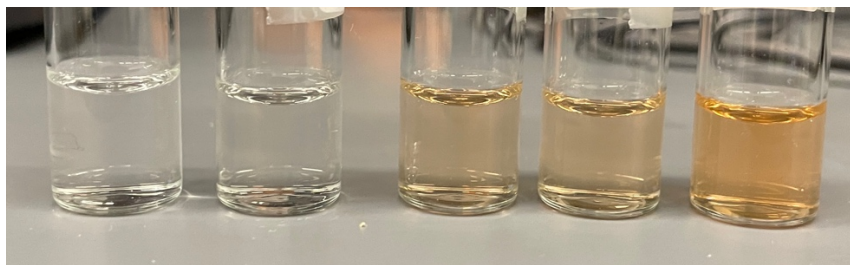


**Figure 4.12.** 2 mL glucose solutions from figure 4.11 after 24 hours. Concentrations from left to right are 0, 0.001, 0.01, 0.1, 0.25 mM.

After 24 hours post-membrane-removal, the glucose solutions appeared to be optically the same intensity, signifying that the colorimetric change in solutions was dictated by exposure to the PEG-PLA membrane. The lack of further color change in the 24-hour period signified that little-to-none of the reaction reagents diffused into the solution and continue after the membrane was removed. Due to the low volume of glucose solutions, UV-vis spectroscopy was not used to analyze these tests due to improper absorbance readings.

Further testing was conducted using 5-mL glucose solutions. Optical results were similar to that of previous testing in that color change was visible after 10 minutes of exposure to the PEG-PLA membrane.

#### **4.5.2 *UV-vis Spectroscopy***

Data using UV-vis was collected for glucose solutions with concentrations of 0 to 1 mM, incremented exponentially. A calibration curve was also collected for 0 mM to 0.1 mM, incremented by 0.02 using the free enzyme and glucose solutions without a membrane-base. The amounts of enzymes and colorimetric agent for the calibration solutions were the same as the amounts used in the PEG-PLA membrane. Figures 4.13 and 4.14 were made using the calibration data collected from UV-vis spectroscopy. Previous

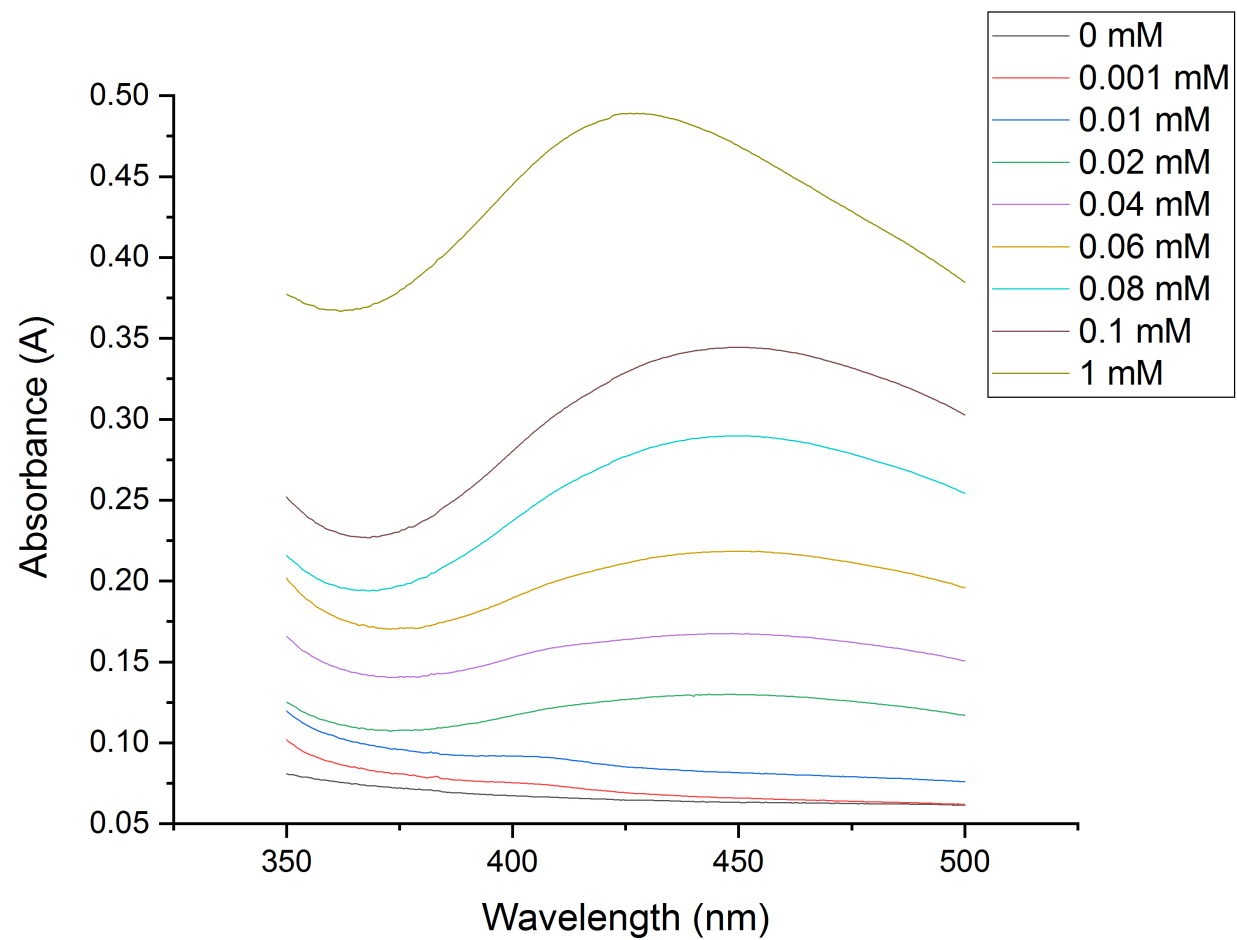


**Figure 4.13.** Absorbance of free-enzyme glucose solutions across wavelength range of 500 to 350 nm for calibration purposes.

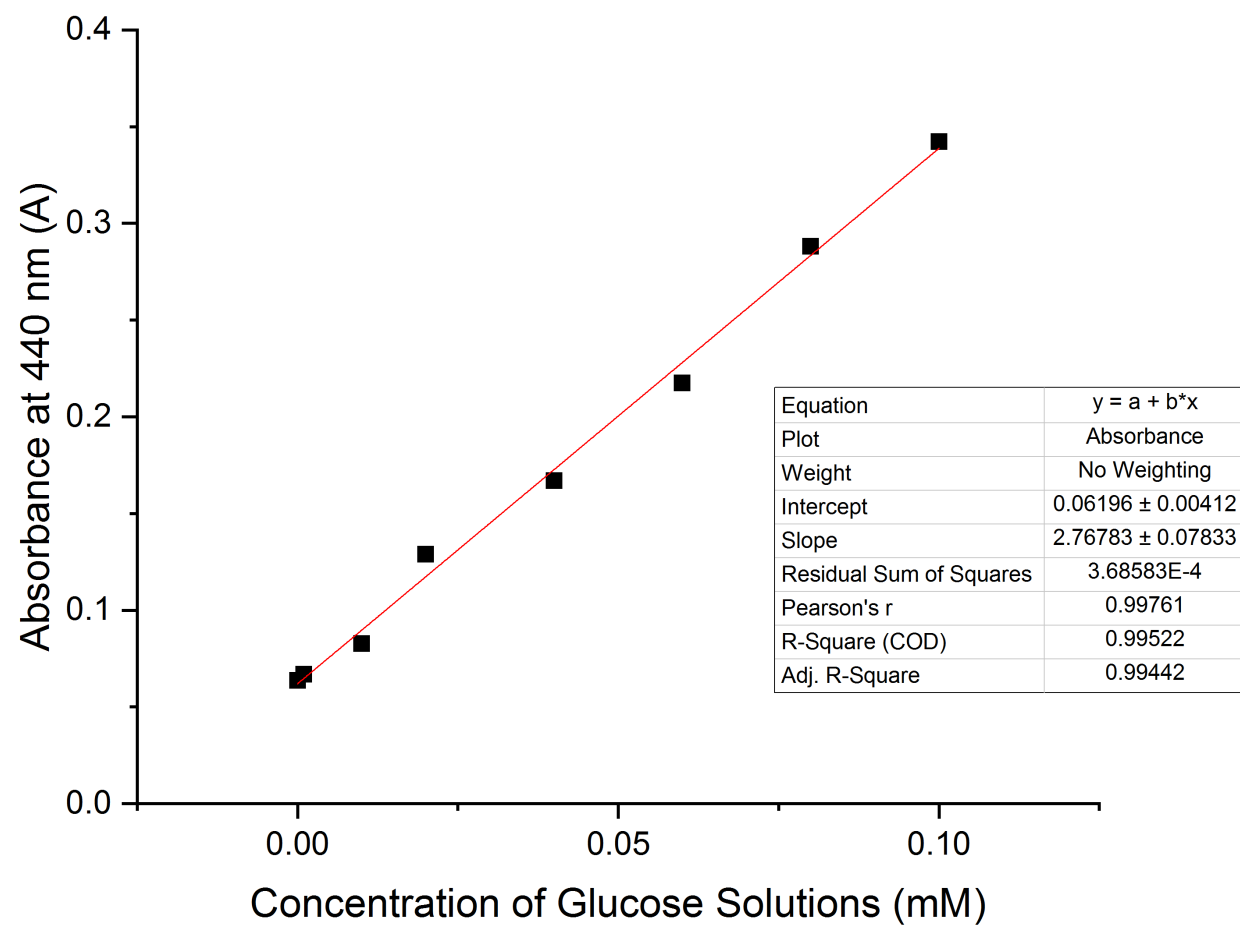


**Figure 4.14.** Calibration curve for absorbance at 440 nm of free-enzyme glucose solution concentrations.

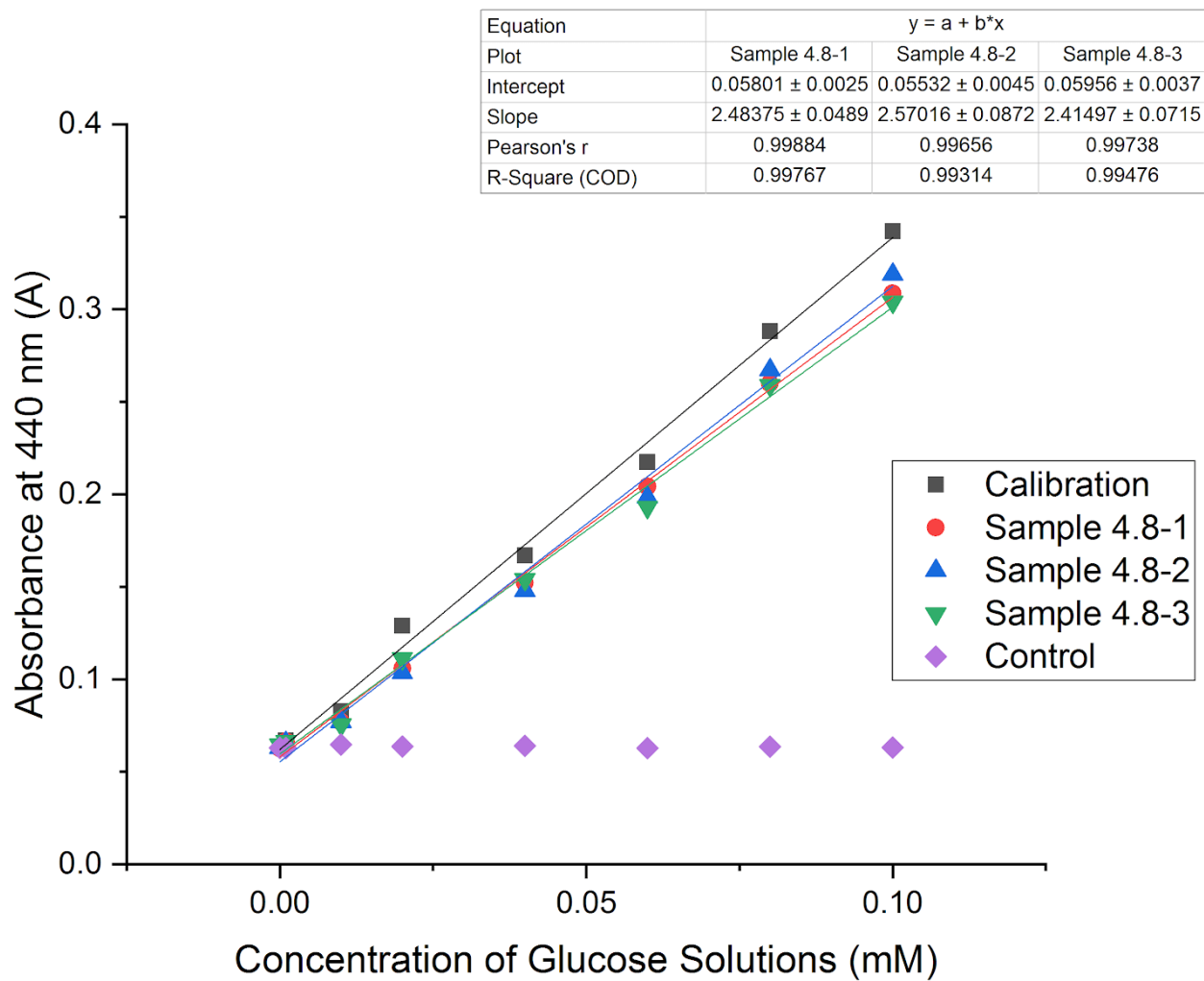


**Figure 4.15.** Absorbance at 440 nm of varying glucose solution concentrations exposed to PEG-PLA membranes.

literature has shown that *o*-dianisidine has maximal absorbance at around 440 nm [12], and the absorbances at this respective wavenumber were plotted for a calibration curve in Figure 4.14. Samples and their storage life between testing can be seen at table 4.8 in the appendix, and their absorbances at 440 nm across glucose solutions can be seen at tables 4.9 and 4.10 in the appendix. It was noted that the wavelength scan for 1 mM in the calibration curve plateaued in absorbance, signifying that this concentration likely was too high for the ratio of mechanism encapsulated in the membrane. With this in mind, the range for 0 to 0.1 mM of glucose concentrations was further examined for its relationship. A control sample, a PEG-PLA membrane without the reaction mechanism, was also tested. Figure 4.15 shows the absorbance at 440 nm of varying glucose concentrations exposed to 3 PEG-PLA membranes and control sample. The control sample had no clear increase in absorbance at 440 nm, signifying that the color change is resulting from the reaction mechanism loaded into the PEG-PLA membrane. Also, the calibration curve itself has an R-squared value of 0.99522, and in comparison to the other R-squared values for the samples from Table 4.8, it was apparent that there is a solid linear relationship between glucose concentration and absorbance at 440 nm. That being said, it was clear from Figure 4.15 that there was a decrease in activity of the reaction once encapsulated in the nanofiber membranes. The slope collected for the calibration curve was shown to be approximately 2.7, and the slopes for the samples measured at 440 nm were approximately 2.4 to 2.5, showcasing that approximately 89.9 percent of the reaction activity is maintained once electrospun. Overall, the data collected in Figure 4.15 attests to the glucose sensing ability of the PEG-PLA bioactive membranes and their potential for clinical applications.

The stability of the PEG-PLA bioactive membrane was also examined by measuring the absorbance of glucose solutions exposed to a 2-month-old PEG-PLA membrane, a 1-month-old PEG-PLA membrane, versus a 24-hour-old PEG-PLA membrane stored at room temperature in Figure 4.16. The calibration curve was also plotted on Figure 4.16 for comparison purposes. Looking at the overall plot, it was clear that the activity of the bioactive membrane diminished after 2-months of storage, most likely due to the instability of the enzymes at ambient room temperature. In past literature, the bienzyme system is best maintained at around 4 degrees Celsius in the context of reaction activity when encapsulated [12]. It was expected that the activity of the membrane would decrease over time when stored at room temperature, and looking at the slopes of the membranes, it was clear that the activity decreased. The relationship between the storage time and activity with respect to the calibration system can be seen in Figure 4.17. Looking at the figure, the 1-day-old sample had an approximate slope of 2.5, the 30-day-old sample has an approximate slope of 2.3, and the 60-day-old sample had a slope of approximately 2.2. Comparing this to the calibration curve, the 30-day and 60-day samples reduced in activity to respectively 83.2% and 78.7%, and with respect to the 1-day-old sample, the 30-day and 60-day samples reduced to respectively 92.7% and 87.7% activity rates. Despite the reduction in activity however, the linear relationship between absorbance and glucose concentration still remained to be strong even after 2 months of storage, as all samples had R-squared values over 0.9.

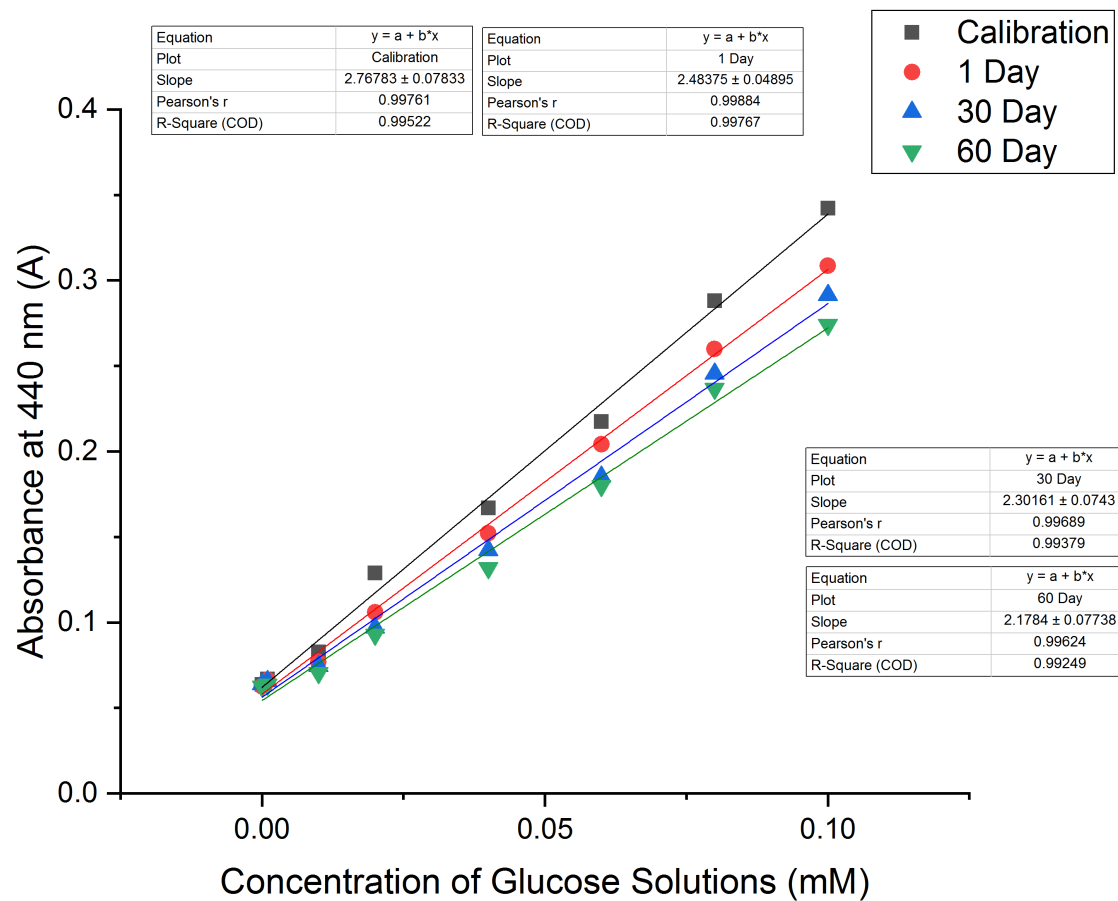


**Figure 4.16.** Absorbance at 440 nm for varying glucose solutions exposed to a 60-day-old, 30-day-old, and 1-day-old PEG-PLA membrane.

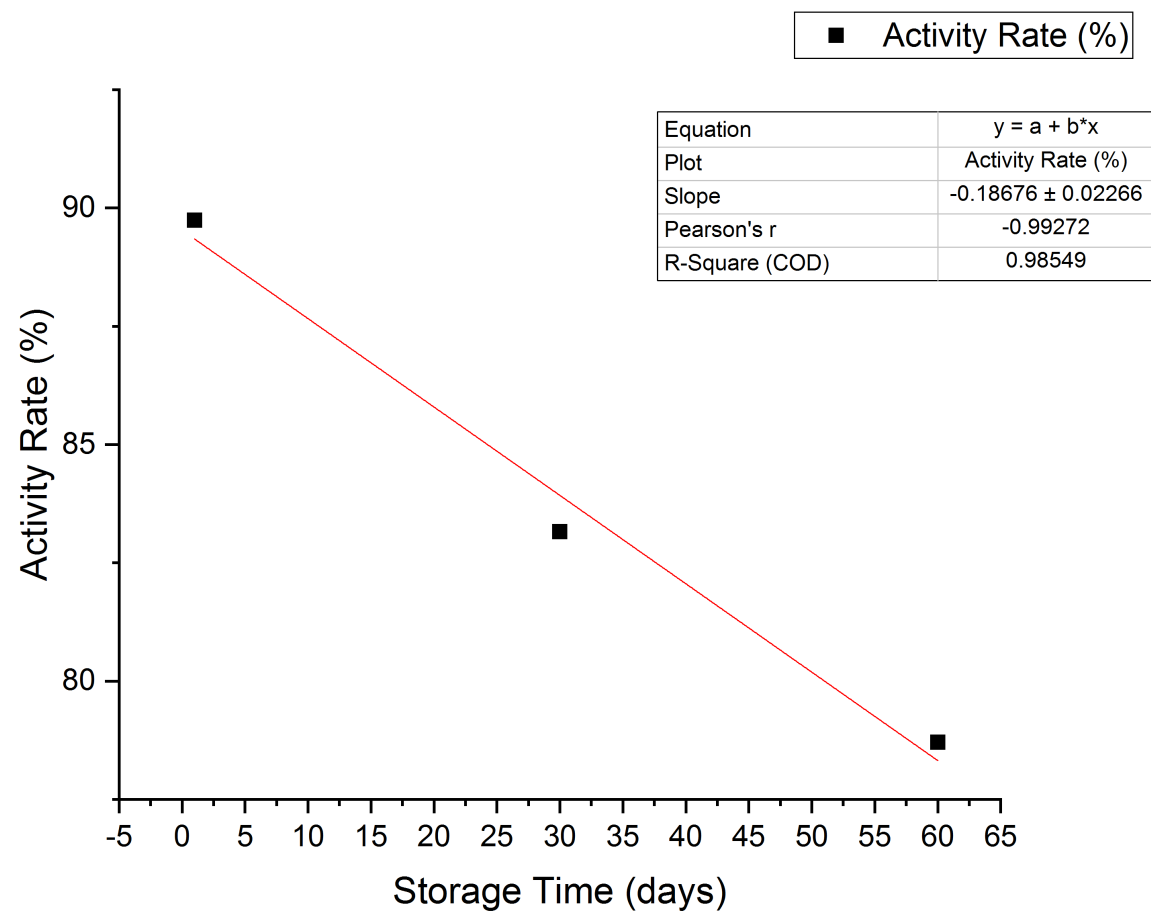


**Figure 4.17.** Activity rate of PEG-PLA membrane samples over storage time.



## **CHAPTER 5**

### **CONCLUSIONS**

Glucose-detecting PLA-PEG core-sheath fiber membranes were fabricated with a bienzyme system, colorimetric agent, and co-axial electrospinning. Co-axial electrospinning parameters were identified to make PEG-PLA bioactive membranes for glucose sensing. The morphology and colorimetric properties of these membranes were investigated and these properties were characterized. Based on the results obtained, the following conclusions are drawn in this research:

1. There was a linear relationship between absorbance at 440 nm and the concentration of glucose solutions . The R-squared values for membranes tested were over 0.9, signifying the presence of this relationship. Increasing the concentration of glucose in solution would increase the absorbance at 400 nm.
2. The activity of the reaction mechanism was reduced to approximately 90% once encapsulated in a PEG-PLA core-sheath membrane when exposed to glucose solutions. This was tabulated in comparison to the free reaction mechanism in glucose solutions of equal bienzyme and colorimetric agents.
3. The limiting reagent in this PEG-PLA membrane for glucose sensing was the concentration of the glucose solutions. This was confirmed in a 24-hour colorimetric test in which the glucose solutions optically increased in color intensity after a 24-hour period of exposure to the membrane.
4. The change in color intensity was relatively dictated by the period of exposure or concentration of glucose exposed to the PEG-PLA membrane. After the PEG-PLA

membranes were removed from the glucose solutions, the color intensity remained optically stable after 24 hours.

5. The electrospinning parameters used for the PEG-PLA bioactive membrane produced core-sheath fibers with a diameter of approximately 15-micron, with the thicknesses of the core and sheath structures being approximately 15 and 10 micron thick.
6. Storing the PEG-PLA membrane at room temperature over time reduced the activity of the membrane. After a storage time of approximately 2 months, the activity of the membranes reduced to 78% in comparison to the free reaction mechanism of the enzymes and colorimetric agent.
7. A linear relationship was maintained between absorbance/color intensity and concentration of glucose after 2 months of storage. The R-squared values for the 2-month-old membranes were over 0.9.

For the results obtained in this thesis, it can be concluded that the PEG-PLA bioactive membranes were successful in colorimetric detection of glucose in solutions by reliance on a bienzyme system and colorimetric agent. It is important to note that the simplicity of co-axial electrospinning and encapsulation in comparison to the other glucose sensor fabrication methods allows for easy modification in the active agent amounts. Further research could include the optimization of the electrospinning process to minimize icing and to increase the limiting reagent, *o*-dianisidine, as well as the reduction of lag-time for colorimetric change in glucose solutions. The PEG-PLA bioactive membranes studied in this thesis have shown significant innovation in electrospun nanofibers as glucose sensors and demonstrate the ability to be used in applications for glucose sensing.

## **CHAPTER 6**

### **FUTURE DIRECTIONS**

This thesis focused on the development and characterization of an electrospun fiber membrane functionalized to colorimetrically detect glucose using a bienzyme system and colorimetric agent. While this thesis introduced the concept using a PEG-PLA core-sheath fiber structure and characterized the spinnability and detection properties of these membranes, there is still much room for further study and optimization. Improvements for further study include the optimization in the loading of the active ingredients for glucose detection as well as applications for detection of glucose in bio-fluids.

In terms of loading of the active ingredients into the polymer solutions, there are two areas that can be considered. The first is the amount of *o*-dianisidine loaded into the sheath polymer solution. As the amount of this colorimetric agent increases, the polymer solution viscosity will also increase due to the suspension of the agent. Future research should look into avenues for maximizing this amount based on the GOx and HRP amounts in the core while minimizing solution viscosity for greater spinnability. Potential solution to this can include examining the use of a larger needle size to adapt to the increased viscosities.

There is also opportunity to explore the applicability of the membrane with glucose-containing bio-fluids. This thesis focused on testing with glucose solutions of varying concentrations in a phosphate buffer saline, thus the room for contaminants and their effect on the membrane was minimal. For applications in the biomedical scene, it is critical to examine and explore potential contaminants that could hinder the performance of the membrane. The membranes can be characterized in this matter by examining the color

change of the membrane itself rather than the fluid of immersion/exposure, as characterizing and standardizing the color of the membrane would be easier. Also, it is ideal for the rate of color change or optical detection for glucose sensing to be minimized. This experiment looked at a 10-minute time frame for exposure to the PEG-PLA bioactive membrane for solid optical results, but in the context of clinical applications, it may be necessary to significantly reduce this time-frame to increase its practicality.

## **APPENDIX**

**Table 4.1.** Electrospun PLA mats of varying concentrations (single-material).

<b>Trial (#)</b>	<b>Concentration of PLA (%)</b>	<b>Observations</b>
1	10	Much spraying, lots of icing at needle tip; ~30% coverage of plate
2	10	Much spraying, lots of icing at needle tip; ~20% coverage of plate
3	12	Good spinning, minimal icing; ~60% coverage of plate
4	12	Good spinning, minimal icing; ~60% coverage of plate
5	15	Great spinning, little-to-no icing; ~90% coverage of plate
6	15	Great spinning, little-to-no icing; ~90% coverage of plate
7	17	Good spinning, minimal icing; ~70% coverage of plate
8	17	Good spinning, minimal icing; ~80% coverage of plate

**Table 4.2.** Electrospun PEG mats of varying concentrations (single-material).

<b>Trial (#)</b>	<b>Concentration of PEG (%)</b>	<b>Observations</b>
1	10	Much spraying, lots of solution drip at needle tip; ~30% coverage of plate
2	10	Much spraying, lots of solution drip at needle tip; ~20% coverage of plate
3	12	Lessened spraying, still lots of solution drip; ~40% coverage of plate
4	12	Lessened spraying, still lots of solution drip; ~40% coverage of plate
5	15	More spinning, but still spraying; ~50% coverage of plate
6	15	More spinning, but still spraying; ~50% coverage of plate
7	17	Better spinning, minimal spraying; ~55% coverage of plate
8	17	Better spinning, minimal spraying; ~55% coverage of plate

**Table 4.3.** Electrospinning 15% PLA solutions with varying parameters (single-material).

<b>Trial (#)</b>	<b>Needle-to-Plate Distance (cm)</b>	<b>Voltage (kV)</b>	<b>Observations</b>
1	12	20	Great spinning, little-to-no icing; ~90% coverage of plate
2	12	20	Great spinning, little-to-no icing; ~90% coverage of plate
3	10	20	Decent spinning, more spraying; ~70% coverage of plate
4	10	20	Decent spinning, more spraying; ~65% coverage of plate
5	15	20	Decent spinning, more icing; ~50% coverage of plate
6	15	20	Decent spinning, more icing; ~50% coverage of plate
7	12	23	Decent spinning, more icing; ~65% coverage of plate
8	12	23	Decent spinning, more icing; ~65% coverage of plate
9	12	15	Great spinning, little-to-no icing; ~95% coverage of plate
10	12	15	Great spinning, little-to-no icing; ~95% coverage of plate

**Table 4.4.** Electrospinning 17% PEG solutions with varying parameters.

<b>Trial (#)</b>	<b>Needle-to-Plate Distance (cm)</b>	<b>Voltage (kV)</b>	<b>Observations</b>
1	12	20	Good spinning, minimal spraying; ~55% coverage of plate
2	12	20	Good spinning, minimal spraying; ~55% coverage of plate
3	10	20	Decent spinning, more spraying; ~30% coverage of plate
4	10	20	Decent spinning, more spraying; ~35% coverage of plate
5	15	20	Decent spinning, much solution drip; ~20% coverage of plate
6	15	20	Decent spinning, much solution drip; ~10% coverage of plate
7	12	23	Much spraying; ~20% coverage of plate
8	12	23	Much spraying; ~20% coverage of plate
9	12	15	Decent spinning, little spraying; ~45% coverage of plate
10	12	15	Decent spinning, little spraying; ~50% coverage of plate



**Table 4.5.** Co-axial electrospinning PLA and PEG solutions.

<b>Trial (#)</b>	<b>Sheath Flow Rate of PLA Solution (mL/hr)</b>	<b>Core Flow Rate of PLA Solution (mL/hr)</b>	<b>Observations</b>
1	1	1	Decent spinning, adequate icing; ~60% coverage of plate
2	1	1	Decent spinning, adequate icing; ~65% coverage of plate
3	1.5	1	Decent spinning, more icing; ~60% coverage of plate
4	1.5	1	Decent spinning, more icing; ~60% coverage of plate
5	2	1	Decent spinning, more icing; ~60% coverage of plate
6	2	1	Decent spinning, more icing; ~50% coverage of plate
7	1	0.85	Great spinning, little-to-no icing; ~95% coverage of plate
8	1	0.85	Great spinning, little-to-no icing; ~95% coverage of plate
9	1	0.75	Great spinning, little-to-no icing; ~95% coverage of plate
10	1	0.75	Great spinning, little-to-no icing; ~95% coverage of plate

**Table 4.6.** Co-axial electrospinning PLA and PEG solutions with fluorescent dyes.

<b>Trial (#)</b>	<b>Sheath Flow Rate of PLA Solution (mL/hr)</b>	<b>Core Flow Rate of PLA Solution (mL/hr)</b>	<b>Observations</b>
1	1	0.75	Great spinning, little-to-no icing; ~95% coverage of plate
2	1	0.85	Great spinning, little-to-no icing; ~95% coverage of plate

**Table 4.7.** Co-axial electrospinning PLA and PEG solutions with HRP, GOx, & *o*-dianisidine.

<b>Trial (#)</b>	<b>Amount of <i>o</i>-Dianisidine to GOx and HRP (mg)</b>	<b>Observations</b>
1	40:5	Little-to-no spinning; lots of clogging/icing
2	40:5	Little-to-no spinning; lots of clogging/icing
3	20:2.5	Good spinning, little icing; ~95% coverage of plate
4	20:2.5	Good spinning, little icing; ~95% coverage of plate
5	30:3.75	Little-to-no spinning, heavy icing
6	30:3.75	Little-to-no spinning, heavy icing

**Table 4.8.** Co-axial electrospinning PEG-PLA membranes for colorimetric testing.

<b>Trial (#)</b>	<b>Approximate Time Interval Between Fabrication and Testing (Days)</b>
1	1
2	1
3	1
4	30
5	60

**Table 4.9.** Absorbance at 440 nm for glucose solutions exposed to 1-day-old PEG-PLA membranes.

Concentration of Glucose Solutions (mM)	Calibration (A)	Control (A)	Trial 1 from Table 4.8 (A)	Trial 2 from Table 4.8 (A)	Trial 3 from Table 4.8 (A)
0	0.0637	0.063012	0.0625621	0.063063	0.0644880
0.001	0.066864	0.0628754	0.0663382	0.0656256	0.0664435
0.01	0.082705	0.0646322	0.0770166	0.0771093	0.0755009
0.02	0.1288216	0.0635906	0.1060065	0.1034301	0.1111594
0.04	0.166874	0.0639806	0.1520204	0.1479727	0.154073
0.06	0.2173636	0.06628661	0.2040845	0.1984100	0.1929084
0.08	0.28807	0.0635886	0.2598786	0.2673549	0.258986
0.1	0.342093	0.0632712	0.3086147	0.3188969	0.3039405

**Table 4.10.** Absorbance at 440 nm for glucose solutions exposed to stored PEG-PLA membranes.

Concentration of Glucose Solutions (mM)	30-days-old (A)	60-days-old (A)
0	0.06385151	0.0625058
0.001	0.06568575	0.0636045
0.01	0.07463121	0.0704028
0.02	0.0969226	0.0929129
0.04	0.1422398	0.1318954
0.06	0.18527609	0.1799318
0.08	0.24554466	0.2365783
0.1	0.2915927	0.2741030

## REFERENCES

- 1) Solomon, S. L., Plisko, J. D., Wittig, S. M., Edwards, L. V., Imhoff, R. H., DiPietro, B., & Plisko, M. J. (2018). Reducing environmental surface contamination in healthcare settings: A statewide collaborative. *American Journal of Infection Control*, 46(8). doi:10.1016/j.ajic.2018.03.016
- 2) Center for Devices and Radiological Health. (n.d.). *Blood Glucose Monitoring Devices*. U.S. Food and Drug Administration. <https://www.fda.gov/medical-devices/in-vitro-diagnostics/blood-glucose-monitoring-devices>.
- 3) Diabetes Research Institute. (2018). *Help for Living with Diabetes*. Living with Diabetes. <https://www.diabetesresearch.org/living-with-diabetes>.
- 4) Senthamizhan, A., Balusamy, B., & Uyar, T. (2015). Glucose sensors based on electrospun nanofibers: a review. *Analytical and Bioanalytical Chemistry*, 408(5), 1285–1306. <https://doi.org/10.1007/s00216-015-9152-x>
- 5) Ginsberg, B. H. (2009). Factors affecting blood glucose monitoring: Sources of errors in measurement. *Journal of Diabetes Science and Technology*, 3(4), 903–913. doi:10.1177/193229680900300438
- 6) Ji, X., Su, Z., Wang, P., Ma, G., & Zhang, S. (2014). “Ready-to-use” hollow nanofiber membrane-based glucose testing strips. *The Analyst*, 139(24), 6467–6473. <https://doi.org/10.1039/c4an01354a>
- 7) Smith, S., Goodge, K., Delaney, M., Struzyk, A., Tansey, N., & Frey, M. (2020). A Comprehensive Review of the Covalent Immobilization of Biomolecules onto Electrospun Nanofibers. *Nanomaterials*, 10(11), 2142. <https://doi.org/10.3390/nano10112142>
- 8) Afshari, M. (2017). In *Electrospun nanofibers*. essay, Elsevier.
- 9) Han, D., & Steckl, A. J. (2019). Coaxial Electrospinning Formation of Complex Polymer Fibers and their Applications. *ChemPlusChem*, 84(10), 1453–1497. <https://doi.org/10.1002/cplu.201900281>
- 10) Kanmaz, D., Aylin Karahan Toprakci, H., Olmez, H., & Toprakci, O. (2018). Electrospun Polylactic Acid Based Nanofibers for Biomedical Applications. *Material Science Research India*, 15(3), 224–240. <https://doi.org/10.13005/msri/150304>
- 11) Ou, K.-L., Chen, C.-S., Lin, L.-H., Lu, J.-C., Shu, Y.-C., Tseng, W.-C., ... Chen, C.-C. (2011). Membranes of epitaxial-like packed, super aligned electrospun

- micron hollow poly(l-lactic acid) (PLLA) fibers. *European Polymer Journal*, 47(5), 882–892. <https://doi.org/10.1016/j.eurpolymj.2011.02.001>
- 12) Lobo, A. O., Afewerki, S., de Paula, M. M., Ghannadian, P., Marciano, F. R., Zhang, Y. S., ... Khademhosseini, A. (2018). Electrospun nanofiber blend with improved mechanical and biological performance. *International Journal of Nanomedicine*, Volume 13, 7891–7903. <https://doi.org/10.2147/ijn.s175619>
  - 13) Mugweru, A., Clark, B. L., & Pishko, M. V. (2007). Electrochemical Sensor Array for Glucose Monitoring Fabricated by Rapid Immobilization of Active Glucose Oxidase within Photochemically Polymerized Hydrogels. *Journal of Diabetes Science and Technology*, 1(3), 366–371. <https://doi.org/10.1177/193229680700100308>
  - 14) Pant, B., Park, M., & Park, S.-J. (2019). Drug Delivery Applications of Core-Sheath Nanofibers Prepared by Coaxial Electrospinning: A Review. *Pharmaceutics*, 11(7), 305. <https://doi.org/10.3390/pharmaceutics11070305>
  - 15) Microfluidic Chip-Based Wearable Colorimetric Sensor for Simple and Facile Detection of Sweat Glucose. <https://doi.org/10.1021/acs.analchem.9b03110.s001>
  - 16) Fang, Y., Zhu, X., Wang, N., Zhang, X., Yang, D., Nie, J., & Ma, G. (2019). Biodegradable core-shell electrospun nanofibers based on PLA and  $\gamma$ -PGA for wound healing. *European Polymer Journal*, 116, 30–37. <https://doi.org/10.1016/j.eurpolymj.2019.03.050>